A Blind Source Separation Technique for Document Restoration Based on Image Discrete Derivative

Antonio Boccuto[1], Ivan Gerace[1(✉)], Valentina Giorgetti[2], and Gabriele Valenti[1]

[1] Dipartimento di Matematica e Informatica, Via Vanvitelli, 1, 06123 Perugia, Italy
{antonio.boccuto,ivan.gerace}@unipg.it
[2] Dipartimento di Matematica e Informatica, viale G. B. Morgagni, 67/A, 50134 Firenze, Italy
valentina.giorgetti@unifi.it

Abstract. In this paper we study a *Blind Source Separation* (BSS) problem, and in particular we deal with document restoration. We consider the classical linear model. To this aim, we analyze the derivatives of the images instead of the intensity levels. Thus, we establish non-overlapping constraints on document sources. Moreover, we impose that the rows of the mixture matrices of the sources have sum equal to 1, in order to keep equal the lightnesses of the estimated sources and those of the data. Here we give a technique which uses the symmetric factorization, whose goodness is tested by the experimental results.

Keywords: Blind source separation · Image restoration · Document restoration · Image derivative · Symmetric factorization

1 Introduction

In this paper we deal with a *Blind Source Separation* (BSS) problem, which is widely studied in signal processing and presents various developments in several areas. We consider both *show-through* and *bleed-through* deteriorations. The show-through is due mostly to the scanning operation. The bleed-through is a physic phenomenon, due to the ink infiltration between the sides of the document.

We analyse a usual linear and stationary recto-verso model (see, e.g., [8–10,16]), and deal with the problem of finding an estimate of the ideal source images of both sides of the document and of the mixture matrix which describes the bleed-through and show-through effects. The BSS problem is ill-posed in the sense of Hadamard (see, e.g., [7]). Indeed, given any mixture matrix, there exists a corresponding pair of ideal images, which are solutions of the problem.

Among the *Independent Component Analysis* (ICA) techniques, many methods are proposed, in which it is supposed to have a mutual independence of

© The Author(s), under exclusive license to Springer Nature Switzerland AG 2022
O. Gervasi et al. (Eds.): ICCSA 2022, LNCS 13375, pp. 445–461, 2022.
https://doi.org/10.1007/978-3-031-10522-7_31

the related sources (see, e.g., [5]). The most used ICA technique is the FastICA method (see, e.g., [8–12]), by means of which it is possible to determine an orthogonal rotation of the data which maximizes non-Gaussianity, using a fixed-point iteration.

Other techniques impose that the estimated sources are mutually uncorrelated. In this case, they are found by a linear transformation of the data, determined by assuming an orthogonality condition, as in *Principal Component Analysis* (PCA), or an orthonormality property, like in *Whitening* (W) and *Symmetric Whitening* (SW) methods (see, e.g., [15,16]).

In [1] a change of variables concerning the data is made, so that the presence and absence of text in the analysed document are associated respectively with high and low intensities of the light, and a nonnegativity constraint concerning the estimated sources is posed (see, e.g., [3,4,6,13]). Moreover, as the lightness of the background of the source is expected to coincide with the lightness of the data, we suppose that all rows of the mixing matrix have sum equal to one.

In [1] the *overlapping matrix* of both the observed data is defined, from which it is possible to deduce the *overlapping level*, which measures the intersections between the letters of the recto and the verso. The technique given in [1] is called *minimum amount of text overlapping in document separation* (MATODS).

In this paper the technique proposed in [1] is modified, and it is dealt with the derivatives of the images of the original sources. In general, the derivatives are related to the edges of the letters contained in the analyzed documents. In particular, we distinguish between horizontal and vertical derivatives. While it is probable that some letters of the recto overlap with some letters of the verso, there is a very low probability that the vertical (horizontal) derivatives of the recto overlap with the vertical (horizontal) derivatives of the verso. Thus, in our proposed technique, we assume that the overlapping level is equal to zero. The knowledge of the overlapping level allows to the proposed technique to eliminate the iterative phase necessary to MATODS to determinate such a level. Thus, it is possible to effectively reduce the computational costs. By means of our experimental results, we show that the proposed technique improves the results obtained in [1] when the source images are noisy. We refer to this method as the *Zero Edge Overlapping in Document Separation* (ZEODS) algorithm.

In Sect. 2 we present the linear model. In Sect. 3 we develop the ZEODS algorithm to deal with the linear problem. In Sect. 4 we compare experimentally the ZEODS algorithm with other fast and unsupervised methods existing in the literature.

2 The Linear Model

The classical linear model is the following (see, e.g., [8–10,14,16]):

$$\widehat{x}^T = A\,\widehat{s}^T, \tag{1}$$

where $\cdot^T$ is the transpose operator, $\widehat{x} \in [0,255]^{nm}$ is the $n \times m$ *data document*, $\widehat{s} \in [0,255]^{nm}$ is the $n \times m$ *source document*, $A \in \mathbb{R}^{2\times 2}$ denotes the *mixture*

matrix. Here we deal with the problem of evaluating the mixture matrix and the ideal sources from the data assuming (1).

However, analogously as in [1], as the paper has the same color for every side of the document, we suppose that the value of the source background is the same as the background of the data. To impose this condition, we require that A is a *one row-sum matrix*, namely

$$a_{11} + a_{12} = a_{21} + a_{22} = 1. \tag{2}$$

Now we introduce a structural modification to the model proposed in [1]. Indeed we will show how, dealing with the first derivatives of the images, the algorithm in [1] will be considerably simplified, reducing computational costs and obtaining significantly better reconstructions in several experimental results. We begin with introducing the concept of *clique* as the set of pixels on which the finite difference of first order is well-defined. The vertical cliques are of the type

$$c = \{(i, j), (i + 1, j)\}, \tag{3}$$

while the horizontal cliques have the form

$$c = \{(i, j), (i, j + 1)\}. \tag{4}$$

We denote by C the set of all cliques. Note that $|C| = 2nm - m - n$, where C denotes the cardinality of C.

Given a vertical clique $c = \{(i, j), (i+1, j)\}$, the finite difference operator on it is $\Delta_c \widehat{\mathbf{x}} = \widehat{x}_{i,j} - \widehat{x}_{i+1,j}$. Moreover, given a horizontal clique $c = \{(i, j), (i, j + 1)\}$, the associated finite difference operator is $\Delta_c \widehat{\mathbf{x}} = \widehat{x}_{i,j} - \widehat{x}_{i,j+1}$. We consider the linear operator $D \in \mathbb{R}^{|C| \times nm}$. Note that, in this matrix, every row index corresponds to a clique, while every column index corresponds to a pixel. To every row it is possible to associate a vertical or horizontal clique. Then, if we consider a vertical clique $c = \{(i, j), (i + 1, j)\}$, we get

$$D_{c,(l,k)} = \begin{cases} 1, & \text{if } (l, k) = (i, j), \\ -1, & \text{if } (l, k) = (i + 1, j), \\ 0, & \text{otherwise;} \end{cases}$$

and, if $c = \{(i, j), (i, j + 1)\}$ is a horizontal clique, we have

$$D_{c,(l,k)} = \begin{cases} 1, & \text{if } (l, k) = (i, j), \\ -1, & \text{if } (l, k) = (i, j + 1), \\ 0, & \text{otherwise.} \end{cases}$$

Let $\dot{x} \in \mathbb{R}^{|C| \times 2}$ be the *data derivative document matrix* defined by

$$\dot{x} = D\widehat{x}. \tag{5}$$

Analogously, the *source derivative matrix* $\dot{s} \in \mathbb{R}^{|C|\times 2}$ is defined by

$$\dot{s} = D\widehat{s}. \tag{6}$$

Notice that the involved images contain letters. If we assume that the colours of the letters and of the background are uniform, then the finite differences are null, while they are different from zero in correspondence with the edges of the letters.

From (1), (5) and (6) we deduce

$$\dot{x}^T = \widehat{x}^T D^T = A\widehat{s}^T D^T = A\dot{s}^T. \tag{7}$$

Note that the linear model obtained by considering the data document derivative matrix and the source derivative matrix is equal to that obtained by treating the data document and the source document in (1).

Analogously as in [1], here we define the following 2×2 *data derivative overlapping matrix* of the observed data:

$$\dot{C} = \begin{bmatrix} \dot{c}_{11} & \dot{c}_{12} \\ \dot{c}_{21} & \dot{c}_{22} \end{bmatrix} = \dot{x}^T \dot{x} = \begin{bmatrix} \dot{x}_r^T \cdot \dot{x}_r & \dot{x}_r^T \cdot \dot{x}_v \\ \dot{x}_v^T \cdot \dot{x}_r & \dot{x}_v^T \cdot \dot{x}_v \end{bmatrix}. \tag{8}$$

The matrix $\dot{C}$ indicates how much the edges of the letters in the front overlap with those of the back. The *source derivative overlapping matrix* can be defined similarly as

$$\dot{P} = \begin{bmatrix} \dot{p}_{11} & \dot{p}_{12} \\ \dot{p}_{21} & \dot{p}_{22} \end{bmatrix} = \dot{s}^T \dot{s} = \begin{bmatrix} \dot{s}_r^T \cdot \dot{s}_r & \dot{s}_r^T \cdot \dot{s}_v \\ \dot{s}_v^T \cdot \dot{s}_r & \dot{s}_v^T \cdot \dot{s}_v \end{bmatrix}.$$

It is not difficult to see that the matrices $\dot{C}$ and $\dot{P}$ are symmetric and positive semidefinite. We refer to the value

$$\dot{k} = \dot{p}_{12} = \dot{p}_{21} = \dot{s}_r^T \cdot \dot{s}_v \tag{9}$$

as the *source derivative overlapping level*. We assume that $\dot{k} = 0$, that is the edges of the recto of the document do not overlap with those of the verso. Note that in [1] the value of the source overlapping level k could not be assumed equal to 0, but could be estimated by searching a fixed point of such a value by means of an iterative method. Such iterative phases caused the algorithm in [1] more computationally expensive than that we are presenting here.

3 A Technique for Solving the Linear Problem

The set of all orthogonal 2×2 matrices is given by the union of all rotations and reflections in $\mathbb{R}^2$, which are expressed as

$$Q^1(\theta) = \begin{bmatrix} \sin\theta & -\cos\theta \\ \cos\theta & \sin\theta \end{bmatrix} \quad \text{and} \quad Q^{-1}(\theta) = \begin{bmatrix} \sin\theta & \cos\theta \\ \cos\theta & -\sin\theta \end{bmatrix}, \tag{10}$$

respectively, as θ varies in $]0, 2\pi]$. As $\dot{C} = \dot{C}^{1/2}(\dot{C}^{1/2})^T = \dot{C}^{1/2}\dot{C}^{1/2}$ is a symmetric factorization of $\dot{C}$, then it is possible to check that all factorizations of $\dot{C}$ have the form

$$Z^{(\iota)}(\theta) = \dot{C}^{1/2} Q^{(\iota)}(\theta) = \begin{bmatrix} \rho_{11} & \rho_{12} \\ \rho_{21} & \rho_{22} \end{bmatrix} Q^{(\iota)}(\theta) = \begin{bmatrix} z_{11}^{(\iota)}(\theta) & z_{12}^{(\iota)}(\theta) \\ z_{21}^{(\iota)}(\theta) & z_{22}^{(\iota)}(\theta) \end{bmatrix}, \tag{11}$$

where $\theta \in]0, 2\pi]$ and $\iota \in \{-1, 1\}$. Moreover, we get

$$z_{11}^{(1)}(\theta) = z_{11}^{(-1)}(\theta),\ z_{12}^{(1)}(\theta) = -z_{12}^{(-1)}(\theta),\ z_{21}^{(1)}(\theta) = z_{21}^{(-1)}(\theta),\ z_{22}^{(1)}(\theta) = -z_{22}^{(-1)}(\theta). \tag{12}$$

We assume that

$$\dot{C} = \dot{x}^T \dot{x} = A\, \dot{s}^T \dot{s}\, A^T = A\, \widetilde{P}\, A^T, \tag{13}$$

where $\widetilde{P}$ denotes a symmetric positive-definite estimate of the source derivative overlapping matrix $\dot{P}$. We put

$$\widetilde{p}_{12} = \widetilde{p}_{21} = 0. \tag{14}$$

Observe that we do not assign a value to $\widetilde{p}_{11}$ and $\widetilde{p}_{22}$, since they will be found later by posing that the estimated mixture matrix is one row-sum. Let us consider

$$\widetilde{P} = YY^T \tag{15}$$

as a symmetric factorization, where Y is a nonsingular matrix fulfilling

$$y_{11}\, y_{21} + y_{12}\, y_{22} = 0, \tag{16}$$

thanks to (14). From (13) and (15) we get

$$\dot{C} = AYY^T A^T = AY(AY)^T,$$

namely AY is a factorization of $\dot{C}$. For each $\theta \in]0, 2\pi]$ and $\iota \in \{-1, 1\}$, we consider an estimate $\widetilde{A}^{(\iota)}(\theta)$ of the mixture matrix A as a matrix with the property that $\widetilde{A}^{(\iota)}(\theta) = Z^{(\iota)}(\theta)Y^{-1}$, with $Z^{(\iota)}(\theta)$ as in (11). We have

$$\begin{aligned} a_{11}^{(\iota)}(\theta) &= \frac{z_{11}^{(\iota)}(\theta)y_{22} - z_{12}^{(\iota)}(\theta)y_{21}}{y_{11}\, y_{22} - y_{21}\, y_{12}}, & a_{12}^{(\iota)}(\theta) &= \frac{z_{12}^{(\iota)}(\theta)y_{11} - z_{11}^{(\iota)}(\theta)y_{12}}{y_{11}\, y_{22} - y_{21}\, y_{12}}, \\ a_{21}^{(\iota)}(\theta) &= \frac{z_{21}^{(\iota)}(\theta)y_{22} - z_{22}^{(\iota)}(\theta)y_{21}}{y_{11}\, y_{22} - y_{21}\, y_{12}}, & a_{22}^{(\iota)}(\theta) &= \frac{z_{22}^{(\iota)}(\theta)y_{11} - z_{21}^{(\iota)}(\theta)y_{12}}{y_{11}\, y_{22} - y_{21}\, y_{12}}. \end{aligned} \tag{17}$$

By requiring that $\widetilde{A}^{(\iota)}(\theta)$ fulfils (2), we get

$$\begin{aligned} z_{11}^{(\iota)}(\theta)y_{22} - z_{12}^{(\iota)}(\theta)y_{21} + z_{12}^{(\iota)}(\theta)y_{11} - z_{11}^{(\iota)}(\theta)y_{12} &= y_{11}\, y_{22} - y_{21}\, y_{12}, \\ z_{21}^{(\iota)}(\theta)y_{22} - z_{22}^{(\iota)}(\theta)y_{21} + z_{22}^{(\iota)}(\theta)y_{11} - z_{21}^{(\iota)}(\theta)y_{12} &= y_{11}\, y_{22} - y_{21}\, y_{12}. \end{aligned} \tag{18}$$

Therefore the matrix Y fulfils properties (16) and (18). The nonlinear system in (16) and (18) admits infinitely many solutions. Among the possible solutions, we take

$$y_{11} = \frac{\det \dot{C}}{(z_{22}^{(\iota)}(\theta) - z_{12}^{(\iota)}(\theta)) \det Z^{(\iota)}(\theta)}, \quad y_{12} = 0, \tag{19}$$

$$y_{21} = 0, \qquad y_{22} = \frac{\det Z^{(\iota)}(\theta)}{z_{11}^{(\iota)}(\theta) - z_{21}^{(\iota)}(\theta)}.$$

Note that, by (12) and (17), we obtain that $\widetilde{A}^{(1)}(\theta) = \widetilde{A}^{(-1)}(\theta)$ for every $\theta \in]0, 2\pi]$. Furthermore, by (10) and (11) we get that $Z(\theta) = -Z(\theta + \pi)$ for any $\theta \in]0, \pi]$, and hence from (17) and (19) we deduce that

$$\widetilde{A}(\theta) = \widetilde{A}(\theta + \pi), \tag{20}$$

for each $\theta \in]0, \pi]$.

So, in the following we deal with the case $\iota = 1$, we put $\widetilde{A}(\theta) = \widetilde{A}^{(1)}(\theta)$ and $Z(\theta) = Z^{(1)}(\theta)$ for each $\theta \in]0, \pi]$.

Note that Y has to be non-singular, since Y is a symmetric factorization of $\dot{P}$.

When the equations in (19) are not defined, that is if $z_{11}(\theta) = z_{21}(\theta)$ or $z_{12}(\theta) = z_{22}(\theta)$, we get that $\theta = \varphi + t\frac{\pi}{2}$, where

$$\varphi = \begin{cases} \arctan\left(\dfrac{\dot{\rho}_{22} - \dot{\rho}_{12}}{\dot{\rho}_{11} - \dot{\rho}_{21}}\right), & \text{if } \dot{\rho}_{11} \neq \dot{\rho}_{21}, \\ \dfrac{\pi}{2}, & \text{if } \dot{\rho}_{11} = \dot{\rho}_{21}, \end{cases} \tag{21}$$

and $\dot{\rho}_{i,j}$, $i, j = 1, 2$, are the entries of the matrix $\dot{C}^{1/2}$.

For every $\theta \in]\varphi, \varphi + \frac{\pi}{2}[\cup]\varphi + \frac{\pi}{2}, \varphi + \pi[$, we get that an estimate of the source derivative matrix $\dot{s}$ is expressed by

$$\widetilde{s}(\theta)^T = \left[\widetilde{s}_r(\theta)\ \widetilde{s}_v(\theta)\right]^T = \widetilde{A}^{-1}(\theta)\dot{x}^T, \tag{22}$$

which, since $\widetilde{A}^{-1}(\theta) = \widetilde{A}^1(\theta) = Z^{(1)}(\theta)Y^{-1}$ and thanks to (18), yields

$$\widetilde{s}_r(\theta) = -\frac{z_{22}(\theta)}{z_{12}(\theta) - z_{22}(\theta)}\dot{x}_r + \frac{z_{12}(\theta)}{z_{12}(\theta) - z_{22}(\theta)}\dot{x}_v; \tag{23}$$

$$\widetilde{s}_v(\theta) = -\frac{z_{21}(\theta)}{z_{11}(\theta) - z_{21}(\theta)}\dot{x}_r + \frac{z_{11}(\theta)}{z_{11}(\theta) - z_{21}(\theta)}\dot{x}_v.$$

Note that the obtained formulas are simpler than the corresponding ones given in [1], because here we consider derivatives of images instead of images. As we supposed that the derivatives of our estimated sources take values between 0 and 2 m, where m is the maximum value of the observed image, we compute the orthogonal projection of $\widetilde{s}(\theta)$ on $[0, 2m]^{nm\times 2}$ related to the Frobenius norm.

We consider the non-negative projections $\tau(\widetilde{s}_{r,\iota}(\theta))$ and $\tau(\widetilde{s}_{v,\iota}(\theta))$ as the new estimates of the derivatives of the sources. Thus we find a value $\widetilde{\theta}$ minimizing the *objective function*

$$g(\theta, \dot{C}) = \tau(\widetilde{s}_r(\theta))^T \cdot \tau(\widetilde{s}_v(\theta)),\ \theta \in]\varphi, \varphi + \frac{\pi}{2}[\cup]\varphi + \frac{\pi}{2}, \varphi + \pi[. \tag{24}$$

Observe that, thanks to (20) and (22), the function g has period π with respect to θ. The function g is minimized by means of the algorithm given in [1].

The proposed algorithm can be written in the following way.

function ZEODS$(\widehat{x})$
$\dot{x} = D\widehat{x}$;
$\dot{C} = \dot{x}^T\dot{x}$;
$\widetilde{\theta} = argmin($**function** $g(\cdot, \dot{C}))$;
$Z(\widetilde{\theta}) = \dot{C}^{1/2}Q_1(\widetilde{\theta})$;
compute $\widetilde{s}_r(\widetilde{\theta})$ and $\widetilde{s}_v(\widetilde{\theta})$ as in (23);
return $D^{-1}\tau(\widetilde{s}(\widetilde{\theta}))$

The function $g(\cdot, \cdot)$ is determined as follows:

function $g(\theta, \dot{C})$
$Z(\theta) = \dot{C}^{1/2}Q^1(\theta)$;
compute $\widetilde{s}_r(\theta)$ and $\widetilde{s}_v(\theta)$ as in (23);
return $(\tau(\widetilde{s}_r(\theta)))^T \cdot \tau(\widetilde{s}_v(\theta))$

We refer to this method as the *Zero Edge Overlapping in Document Separation* (ZEODS) algorithm. Note that ZEODS is an unsupervised technique.

4 Experimental Results

In our experimental results we use quite noisy ideal sources, from which the observed documents are synthetically constructed from suitable mixture matrices. We examine RGB color images. The channels R, G and B are treated separately.

The first case we investigate is a symmetric mixture matrix. For each channel R, G and B, the related matrices are

$$A_R = \begin{pmatrix} 0.6 & 0.4 \\ 0.4 & 0.6 \end{pmatrix},\ A_G = \begin{pmatrix} 0.6 & 0.4 \\ 0.4 & 0.6 \end{pmatrix},\ A_B = \begin{pmatrix} 0.6 & 0.4 \\ 0.4 & 0.6 \end{pmatrix}. \tag{25}$$

Now we see the behavior of the presented algorithms. We consider the ideal images in Fig. 1, and using the above indicated mixture matrices, we synthetically obtain the degraded images in Fig. 2.

By applying the algorithms we get, as estimates, the results in Figs. 3, 4, 5, 6, 7 and 8.



(a) original recto (b) original verso

Fig. 1. Ideal images



(a) degraded recto (b) degraded verso

Fig. 2. Degraded images



(a) recto estimated by ZEODS (b) verso estimated by ZEODS

Fig. 3. Estimates by ZEODS



(a) recto estimated by MATODS (b) verso estimated by MATODS

Fig. 4. Estimates by MATODS



(a) recto estimated by FastIca



(b) verso estimated by FastIca

Fig. 5. Estimates by FastIca



(a) recto estimated by Symmetric Whitening



(b) verso estimated by Symmetric Whitening

Fig. 6. Estimates by Symmetric Whitening



(a) recto estimated by Whitening



(b) verso estimated by Whitening

Fig. 7. Estimates by Whitening

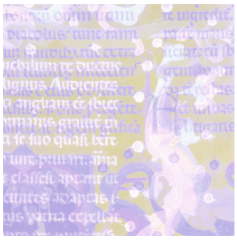

(a) recto estimated by PCA



(b) verso estimated by PCA

Fig. 8. Estimates by PCA

Table 1. Errors of the estimations of the document in Fig. 1 degraded by the mixture matrix in (25).

Used technique	MSE Recto	MSE Verso	MSE of A
ZEODS	5.0766	0.6228	$1.020 \cdot 10^{-4}$
MATODS	12.5173	49.0506	0.0011
FASTICA	58.2382	212.8663	0.0546
Symmetric whitening	428.0422	373.6753	0.00183
Whitening	$7.7086 \cdot 10^3$	$6.2362 \cdot 10^3$	0.3561
PCA	$1.4943 \cdot 10^4$	$5.2861 \cdot 10^3$	0.3770

In Table 1 we present the mean square errors with respect to the original documents obtained by means of the aforementioned algorithms for estimating the recto and the verso of Fig. 1.

We now present the next case. For every channel R, G and B, we consider the following mixture matrices.

$$A_R = \begin{pmatrix} 0.7 & 0.3 \\ 0.2 & 0.8 \end{pmatrix}, \; A_G = \begin{pmatrix} 0.45 & 0.55 \\ 0.4 & 0.6 \end{pmatrix}, \; A_B = \begin{pmatrix} 0.7 & 0.3 \\ 0.51 & 0.49 \end{pmatrix}. \tag{26}$$

Now we see the behavior of the presented algorithms, regarding both errors and the visual point of view. We consider the ideal images in Fig. 9. Using the above indicated mixture matrices, we synthetically obtain the degraded images in Fig. 10. By applying the algorithms we obtain, as estimates, the results in Figs. 11, 12, 13, 14, 15 and 16. In Table 2 we present the mean square errors with respect to the original documents obtained by means of the above algorithms for the estimate of the recto and the verso of Fig. 9.

Finally, we present the results related to the following images in Fig. 17. For the channels R, G and B, we deal again with the mixture matrices in (26).

Using the abovementioned mixture matrices, we synthetically get the degraded images in Fig. 18.

By means of the algorithms we get, as estimates, the results in Figs. 19, 20, 21, 22, 23 and 24.



(a) original recto (b) original verso

Fig. 9. Ideal images

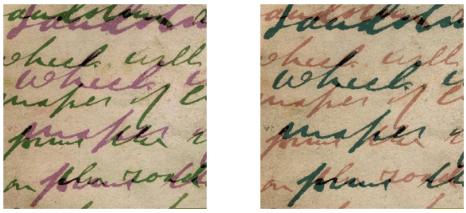

(a) degraded recto (b) degraded verso

Fig. 10. Degraded images

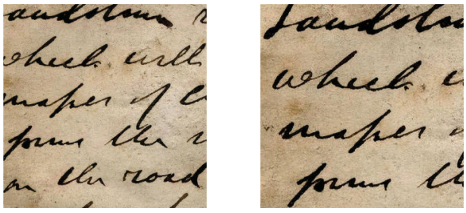

(a) recto estimated by ZEODS (b) verso estimated by ZEODS

Fig. 11. Estimates by ZEODS

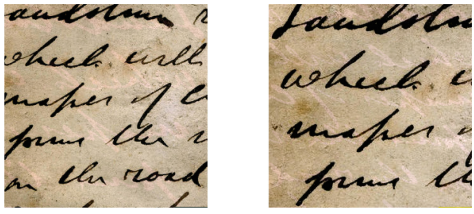

(a) recto estimated by MATODS (b) verso estimated by MATODS

Fig. 12. Estimates by the algorithm MATODS given in [1]

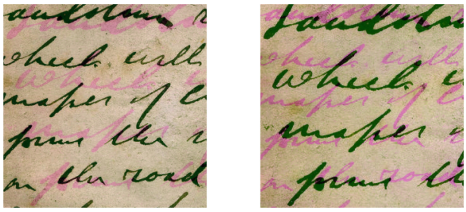

(a) recto estimated by FastICA (b) verso estimated by FastICA

Fig. 13. Estimates by the algorithm FastICA given in [10]

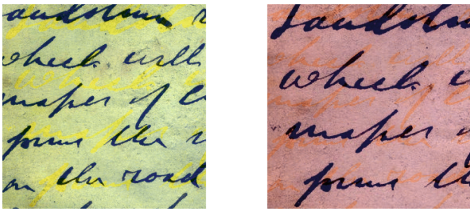

(a) recto estimated by Symmetric Whitening (b) verso estimated by Symmetric Whitening

Fig. 14. Estimates by Symmetric Whitening given in [16]



(a) recto estimated by Whitening (b) verso estimated by Whitening

Fig. 15. Estimates by Whitening given in [16]

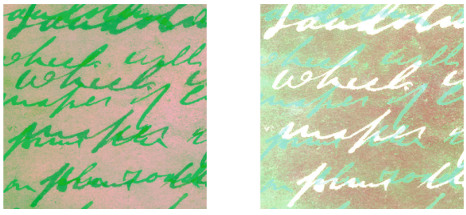

(a) recto estimated by PCA (b) verso estimated by PCA

Fig. 16. Estimates by PCA given in [16]

Table 2. Errors of the estimations of the document in Fig. 9 degraded by the mixture matrix in (26).

Used technique	MSE Recto	MSE Verso	MSE of A
ZEODS	1.2642	2.6337	$2.2806 \cdot 10^{-5}$
MATODS	62.2418	85.4395	0.0026
FastICA	353.226	182.7357	0.0303
Symmetric Whitening	409.8490	495.5137	0.1435
Whitening	$7.7216 \cdot 10^{3}$	$3.5975 \cdot 10^{3}$	0.4449
PCA	$1.2810 \cdot 10^{4}$	$2.5195 \cdot 10^{3}$	0.4473

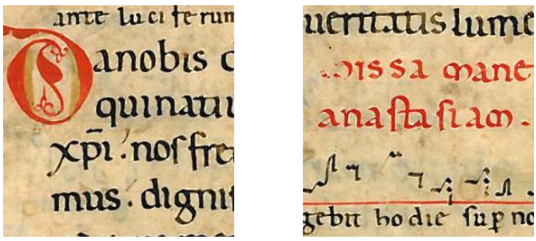

(a) original recto (b) original verso

Fig. 17. Ideal images



(a) degraded recto (b) degraded verso

Fig. 18. Degraded images

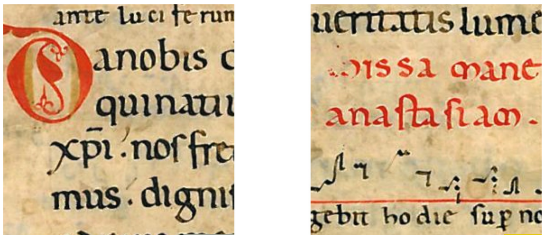

(a) recto estimated by ZEODS (b) verso estimated by ZEODS

Fig. 19. Estimates by ZEODS

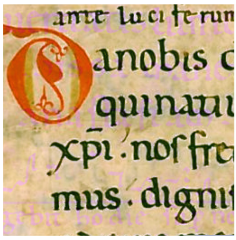

(a) recto estimated by MATODS

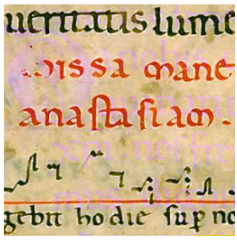

(b) verso estimated by MATODS

Fig. 20. Estimates by MATODS

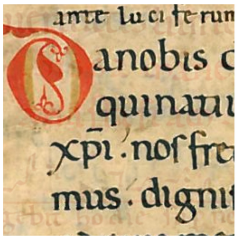

(a) recto estimated by FastIca

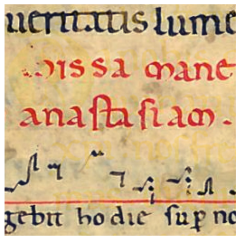

(b) verso estimated by FastIca

Fig. 21. Estimates by FastIca

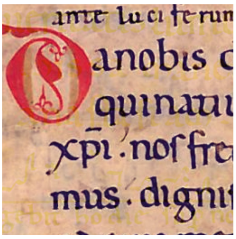

(a) recto estimated by Symmetric Whitening

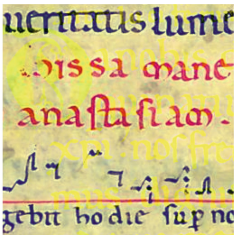

(b) verso estimated by Symmetric Whitening

Fig. 22. Estimates by Symmetric Whitening



(a) recto estimated by Whitening

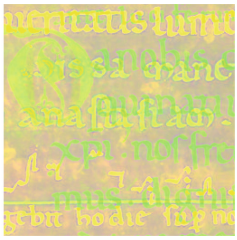

(b) verso estimated by Whitening

Fig. 23. Estimates by Whitening



(a) recto estimated by PCA



(b) verso estimated by PCA

Fig. 24. Estimates by PCA

In Table 3 there are the mean square errors with respect to the original documents obtained using the above algorithms for the estimate of the recto and the verso of Fig. 17.

Table 3. Errors of the estimations of the document in Fig. 17 degraded by the mixture matrix in (26).

Used technique	MSE Recto	MSE Verso	MSE of A
ZEODS	3.2977	3.6252	$1.090 \cdot 10^{-4}$
MATODS	35.0124	42.8569	$1.5041 \cdot 10^{-4}$
FASTICA	232.7229	147.4355	0.0304
Symmetric Whitening	235.6894	607.9245	0.1441
Whitening	$1.4669 \cdot 10^{4}$	$6.6340 \cdot 10^{3}$	0.5272
PCA	$1.9414 \cdot 10^{4}$	$3.9348 \cdot 10^{3}$	0.4795

It is possible to note how the here proposed ZEODS algorithm obtains always results which are qualitatively and quantitatively better than algorithms which assume the same linear model.

In [2] we examined various other cases, in which the ideal sources are quite noisy images, and in almost all studied situations we get the same results, and the better results are obtained by the ZEODS method.

Conclusions

In this article we extended the MATODS method proposed in [1] for the restoration of documents corrupted by bleed-through and/or show-through. In particular, instead of analyzing the gray level of the observed images, we studied the derivatives of the gray level in those images. In this case, there is a very low probability that the horizontal (or vertical) derivatives of the recto overlap with the respective ones of the verso. Thus, differently from the MATODS, the overlapping level is established to be equal to zero. Therefore, no iterative phase is necessary to estimate such a level. Experimentally, we showed that the proposed method is more efficient than MATODS when the original sources are noisy images.

We are preparing an extension of the ZEODS method, to include the case in order to treat the not invariant translation case, similarly to that proposed by the NIT-MATODS (Not Invariant Translation MATODS) ([1]), to deal with real documents.

Acknowledgments. This work was partially supported by University of Perugia, G.N.A.M.P.A. (Italian National Group of Mathematical Analysis, Probability and Applications) and I.N.d.A.M. (Italian National Institute of Higher Mathematics).

References

1. Boccuto, A., Gerace, I., Giorgetti, V.: A blind source separation technique for document restoration. SIAM J. Imaging Sci. **12**(2), 1135–1162 (2019)
2. Boccuto, A., Gerace, I., Giorgetti, V., Valenti, G.: A Blind Source Separation Technique for Document Restoration Based on Edge Estimation. http://viXra.org/abs/2201.0141 (2022)
3. Chan, T.-H., Ma, W.-K., Chi, C.-Y., Wang, Y.: A convex analysis framework for blind separation of non-negative sources. IEEE Trans. Signal Process. **56**(10), 5120–5134 (2008)
4. Cichocki, A., Zdunek, R., Amari, S.-I.: New algorithms for non-negative matrix factorization in applications to blind source separation. In: Proceedings of the 2006 IEEE International Conference Acoustics, Speech and Signal Processing, Toulouse, France, pp. 1–4 (2006)
5. Comon, P.: Independent component analysis, a new concept? Signal Process. **36**, 287–314 (1994)
6. Gillis, N.: Successive nonnegative projection algorithm for robust nonnegative blind source separation. SIAM J. Imaging Sci. **7**(2), 1420–1450 (2014)
7. Gillis, N.: Sparse and unique nonnegative matrix factorization through data preprocessing. J. Mach. Learn. Res. **13**, 3349–3386 (2012)
8. Hyvärinen, A.: Fast and robust fixed-point algorithms for independent component analysis. IEEE Trans. Neural Netw. **10**(3), 626–634 (1999)

9. Hyvärinen, A.: The fixed-point algorithm and maximum likelihood estimation for independent component analysis. Neural Process. Lett. **10**(1), 1–5 (1999)
10. Hyvärinen, A., Oja, E.: A fast fixed-point algorithm for independent component analysis. Neural Comput. **9**(7), 1483–1492 (1997)
11. Khaparde, A., Madhavilatha, M., Manasa, M.B.L., Pradeep Kumar, S.: FastICA algorithm for the separation of mixed images. WSEAS Trans. Signal Process. **4**(5), 271–278 (2008)
12. Malik, R. K., Solanki, K.: FastICA based blind source separation for CT imaging under noise conditions. Int. J. Adv. Eng. Technol. **5**(1), 47–55 (2012)
13. Ouedraogo, W.S.B., Souloumiac, A., Jaidane, M., Jutten, C.: Non-negative blind source separation algorithm based on minimum aperture simplicial cone. IEEE Trans. Signal Process. **62**(2), 376–389 (2014)
14. Tonazzini, A., Gerace, I., Martinelli, F.: Multichannel blind separation and deconvolution of images for document analysis. IEEE Trans. Image Process. **19**(4), 912–925 (2010)
15. Tonazzini, A., Gerace, I., Martinelli, F.: Document image restoration and analysis as separation of mixtures of patterns: from linear to nonlinear models. In: Gunturk, B.K., Li, X. (eds.) Image Restoration - Fundamentals and Advances, pp. 285–310. CRC Press, Taylor and Francis, Boca Raton (2013)
16. Tonazzini, A., Salerno, E., Bedini, L.: Fast correction of bleed-through distortion in greyscale documents by a blind source separation technique. Int. J. Doc. Anal. **10**(1), 17–25 (2007)
17. Vavasis, S.: On the complexity of nonnegative matrix factorization. SIAM J. Optim. **20**(3), 1364–1377 (2009)